Smart Structures and Systems, *Vol. 14, No. 2 (2014) 105-128*
DOI: http://dx.doi.org/10.12989/sss.2014.14.2.105

Stochastic DLV method for steel truss structures: simulation and experiment

Yonghui An*[1], Jinping Ou[1], Jian Li[2] and B.F. Spencer Jr.[3]

[1]*Department of Civil Engineering, Dalian University of technology, Dalian, China*
[2]*Department of Civil, Environmental, and Architectural Engineering, University of Kansas, Lawrence, KS, USA*
[3]*Department of Civil and Environmental Engineering, University of Illinois at Urbana-Champaign, Urbana, IL, USA*

(Received February 1, 2012, Revised June 1, 2013, Accepted June 28, 2013)

Abstract. The stochastic damage locating vector (SDLV) method has been studied extensively in recent years because of its potential to determine the location of damage in structures without the need for measuring the input excitation. The SDLV method has been shown to be a particularly useful tool for damage localization in steel truss bridges through numerical simulation and experimental validation. However, several issues still need clarification. For example, two methods have been suggested for determining the observation matrix C identified for the structural system; yet little guidance has been provided regarding the conditions under which the respective formulations should be used. Additionally, the specific layout of the sensors to achieve effective performance with the SDLV method and the associated relationship to the specific type of truss structure have yet to be explored. Moreover, how the location of truss members influences the damage localization results should be studied. In this paper, these three issues are first investigated through numerical simulation and subsequently the main results are validated experimentally. The results of this paper provide guidance on the effective use of the SDLV method.

Keywords: stochastic damage locating vector (SDLV) method; sensor layout; damage detection; steel-truss bridge; damage localization; structural health monitoring

1. Introduction

Structural health monitoring (SHM) is the technique of assessing the health status of a structure using the data obtained from a number of sensors. It aims to perform a diagnosis of the structural safety (Yu and Giurgiutiu 2005) and is capable of detecting, locating, and quantifying different types of damage. It offers the potential for real-time and periodic safety assessment of the civil infrastructure and other mechanical systems (Gao 2005). Damage detection and localization are the key issues of SHM. Even though civil structures are normally designed to last for decades, overloads, excessive usage, exposure to extreme weather, and other unexpected factors can cause rapid deterioration (Kim and Melhem 2004). Existence of damage may influence the performance of the structures or even lead to disaster (Chen and Nagarajaiah 2008). Critical regions in civil

*Corresponding author, E-mail: anyh03@lzu.cn

http://www.techno-press.org/?journal=sss&subpage=8 ISSN: 1738-1584 (Print), 1738-1991 (Online)

infrastructures need real-time diagnosis of initial damage detection and localization, then quantitative severity assessment (Zhou *et al*. 2007). The effective measures to monitor and assess the security situation, repair, and control damage must be adopted immediately on many employed civil infrastructures (Ou 2005).

For several decades from the early work of Lifshitz and Rotem (1969), especially in the past decade, considerable researchers have studied the vibration-based structural damage detection techniques (Hu *et al.* 2001, Yan *et al.* 2007, Balmès *et al.* 2008, Deraemaeker *et al.* 2010, An and Ou 2012). There are many different bases for damage detection methods. Some methods are based on the difference of mode shapes in which the entire structure is monitored by several evenly distributed accelerometers, the general damaged positions are then obtained (Pandey *et al.* 1991). Some other methods are based on the difference of modal strain energy (Shi, *et al.* 2000). Besides these methods, the technique based on the flexibility (Pandey and Biswas 1996) matrix has attracted considerable attention. In 2002, Bernal (2002) proposed the damage locating vector (DLV) method, named the DLV method, based on the flexibility matrix. Gao *et al.* (Gao 2005, Gao *et al.* 2007) verified this method based on the experimental data of a laboratorial truss model. The DLV method requires the input excitations. However, it is not easy to measure inputs of a real structure under ambient excitation, limiting the application of the DLV method. In 2006, Bernal (2006) proposed the DLV method under stochastic random excitation, named the Stochastic DLV method (SDLV), which solves the applications of the DLV method under ambient excitation. It provides an important support for the application in structural health monitoring. The SDLV method is greatly advantageous in the damage detection of truss structures because it can locate the damaged members directly.

However, there are many challenges to be addressed. Firstly, false positive detections were presented in the early work (Gao 2005) although all nodes were measured in the detected substructure, therefore, the issue on improving the accuracy of localization results is worthy of further study. Nagayama *et al.* (2009) described two methods to construct the observation matrix C based on the modal parameters. On the basis of this work, the issue on how to improve the accuracy of localization results through appropriate formulation of the observation matrix C is addressed. Secondly, the SDLV method can detect not only the entire structure but a local substructure (Gao 2005, Nagayama *et al.* 2009). It can be used as a local-identification technique for a truss substructure, so as to decrease the number of sensors. Additionally, the specific layout of the sensors to achieve effective performance with the SDLV method and the associated relationship to the specific type of truss structure have yet to be explored. In general, costs of SHM system (such as costs of data acquisition system and maintenance) increase dramatically with the increase of the number of sensors. Therefore, determining how to detect more elements using fewer sensors has become a very important and challenging issue. Thirdly, how the location of a truss member influences the damage localization result will be summarized.

Considering that a lot of bailey steel-truss bridges are employed in the highway and railway bi-purpose bridges in China, a laboratorial simply-supported steel-truss bridge model based on the bailey steel-truss bridges, which allows easy simulation of various damage cases, has been built in Dalian University of Technology (DUT) for bridge health monitoring study,. To address the above issues, this paper selects the "DUT steel-truss bridge benchmark model" and other common types of truss structure as the research objects. The selection technique of C matrix and the threshold limit of weighted stress index and the sensitivities of the SDLV method to different types of truss members are discussed. The strategies of sensor layout based on the SDLV method used in

different structures are investigated respectively. The results and analysis of both simulation and experiment are given.

2. Fundamental theory of the SDLV method

The stochastic damage locating vector method (SDLV) is the extension of the DLV method when the input is unknown. According to Bernal (2006), when the input excitation is unknown, the null space of the change in the flexibility matrix will be contained in the null space of ΔQ^T, which is the transpose of the change in Q

$$Q = -CA^{-(p+1)}H_P^{\dagger}L = -CA^{-(p+1)}\begin{bmatrix} CA^{1-p} \\ CA^{-p} \end{bmatrix}^{\dagger}\begin{bmatrix} I \\ 0 \end{bmatrix} \tag{1}$$

where A is the system matrix and C is the observation matrix; both of which are identified from vibration measurements; P (= 0, 1, or 2) is the measured displacement, velocity, and acceleration; and † denotes pseudoinverse.

The singular value decomposition of ΔQ^T is employed, and then the null vectors of ΔQ^T are treated as DLVs (Bernal 2002, 2006). The number of SDLV vectors, q, can be determined as follows (Bernal 2006)

$$q = 0.5 * \left\{ number\ of\ \gamma\ values \le 0.1 \,|\, \gamma = \sqrt{\frac{S_i}{S_{i,\max}}} \right\} \tag{2}$$

where S_i are singular values of ΔQ.

Finally, multiple SDLVs are combined to locate damage. The weighted stress index, *WSI*, is introduced, and the elements whose weighted stress index meets the following formula are denoted as a damaged element

$$WSI = \sum_{j=1}^{q} R_i \frac{\left|\sigma_j\right|}{\left|\sigma_j\right|_{\max}} \le b \tag{3}$$

where σ_j is the characterizing stress; Bernal (2006) suggested that $R = 1$ and $b = 0.1$.

3. Numerical and experimental design

To study the selection of C matrix and suitable strategies of sensor layout, a simply supported bailey steel-truss bridge model based on the highway and railway bi-purpose steel truss bridges employed in China has been employed here.

3.1 Description of the bridge model

This model (Fig. 1) was first introduced in the work by An and Ou (2010), and is also

introduced briefly herein for completeness. The span, width, and height are 8 m, 0.56 m, and 0.9 m, respectively. To simulate the structural damage without dissembling the entire structure, the model (Fig. 1) is fabricated by 312 tubes, 108 bolt-sphere joints and 624 bolts without welding. Every truss tube can be loosened, notched, and replaced easily, which conveniently simulates various damage types.

3.2 Finite element modeling

The process of finite element modeling for this model has been introduced in the early studies (An and Ou 2013). A finite element (FE) model (Fig. 2) consisting of 312 beam elements and 108 nodes has been developed with MATLAB (Mathwork Inc. 2005). The element stiffness and mass matrices are derived to form global stiffness and mass matrices in the FE model. As a result, the first two vertical frequencies (19.1 and 52.5 Hz) of the numerical model are very close to the experimental results (18.4 and 53.3 Hz) based on the NExT (James *et al.* 1995) and the ERA (Juang and Pappa 1985) methods.

4. Main focus 1: A further study about the formulation of *C* matrix

Nagayama *et al.* (2009) provided two methods to construct the observation matrix *C*. One is to formulate *C* matrix based on modal parameters

$$C = [\varphi_1 \ \varphi_2 ... \varphi_n \ \varphi_1^* \ \varphi_2^* ... \varphi_n^*] \tag{4}$$

in which φ_1^* is the conjugate complex of φ_1. The other formulation is

$$C = [\varphi_1 \ \varphi_2 ... \varphi_n \ 0 \ 0 ... 0] \tag{5}$$

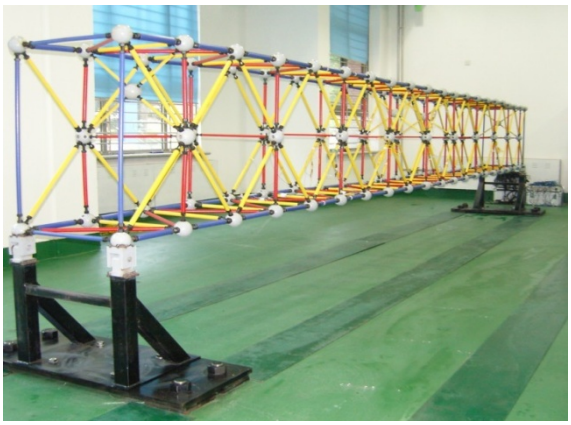

Fig. 1 The steel truss bridge model

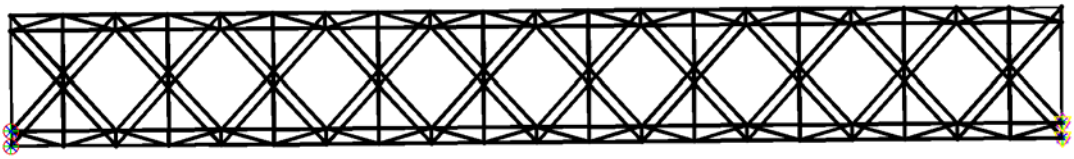

Fig. 2 FE model in MATLAB

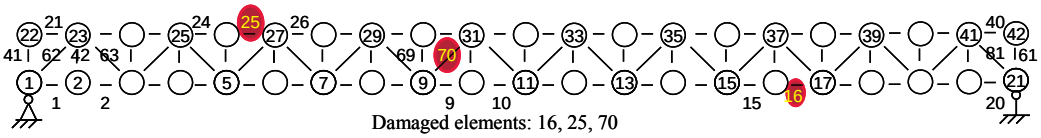

Fig. 3 Truss 1 and Damage case 1

In the study of damage detection in substructures of a truss structure, Nagayama *et al.* (2009) concluded from numerical simulation that the *C* matrix formulation in Eq. (5) gives more accurate damage detection results than using Eq. (4). This paper continues to discuss the selection of *C* matrix based on the above study (Nagayama *et al.* 2009) in the interest of improving the accuracy of damage localization results. To avoid the effect of a particular structural geometry, damage detection of two common truss structures using the SDLV method are simulated (Truss 1 is shown in Fig. 3, Truss 2 is shown in Fig. 7 from the experimental model as described in preceding section).

4.1 Effect of C matrix formulation on damage detection for entire structure

The FE model of Truss 1 is also developed using MATLAB. Damage case 1 is shown in Fig. 3, here elements 16, 25 and 70 in the ellipse are damaged with 50% stiffness reduction, which simulates the damage of the lower chord, the upper chord and the diagonal truss member, respectively. All nodes except the four nodes located at the corners (Fig. 3) are selected as measurements to detect damages in the structure. The bidirectional accelerations of the 38 measurements before and after damage are obtained from their Simulink models. The truss is excited using a band-limited white noise up to 200 Hz in the vertical direction. The sampling frequency is 500 Hz. 5% noise is added to measurements.

In order to compare the results between Eqs. (4) and (5), the standard which defines a better result must be considered. A damage detection result must meet the following requirements in order to be considered as a "better" result: (1) the damaged elements should be detected successfully in the result; (2) the result should have a fewer number of false positive elements; (3) if the first two requirements have been met, when comparing the damage detection results between the two *C* matrix formulations, consider ten threshold $\sigma_{\text{threshold}}$ taking values from the threshold *b* (see Eq. (3)) from 0.1 to 1 with an interval of 0.1, then two numbers are defined including: 1) P_u is the total number of undamaged elements that have smaller stress than every threshold $\sigma_{\text{threshold}}$ in a result; 2) when every threshold $\sigma_{\text{threshold}}$ is employed, *d* is the number of damaged elements that

have larger stress than the other result, and P_d of is the total number of d, i.e. $P_d = 10d$. As a result, $P = P_u + P_d$. A lower value of P is considered a better result. Simulation results (as shown in Fig. 4) of Truss 1 for Damage case 1 showed that C matrix formulation in Eq. (4) gives better results than Eq. (5) for detecting the damage of the entire structure. The conclusion holds true for both Truss 1 and 2.

4.2 Effect of C matrix formulation on damage detection for substructures

Here, substructures of Truss 1 and Truss 2 are selected as detection objects. To find out what parameters of the substructures are affecting the performance of the two C matrix formulations, three potential parameters are investigated including: (1) the percentage of measured bays with respect to the total number of bays in the truss; (2) the percentage of measured tubes and (3) the percentage of measured nodes. Two cases are investigated when (1) all nodes in the substructure are measured and (2) limited nodes are measured. However, it is found that the first two parameters do not give consistent result in terms of the performance of the two C matrix formulations for these two cases. Taking Truss 1 for example, as shown in Table 1, when the first two parameters are 45% and 34.57% respectively, Eq. (4) gives better results in case 1 while Eq. (5) gives better results in case 2. As a result, among these three parameters, the third parameter - the percentage of measured nodes within a substructure - is found to be sensitive to damage detection result when different C matrix formulation is selected among Eqs. (4) and (5). Taking a two-bay substructure and a six-bay substructure (Fig. 5(e)) for example, some typical simulation results are shown in Figs. 5(a)-5(d).

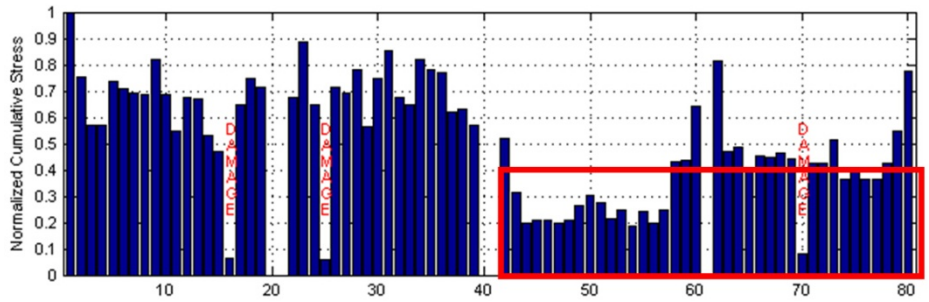

(a) Result of Damage case 1 with C matrix formulation in Eq. (4)

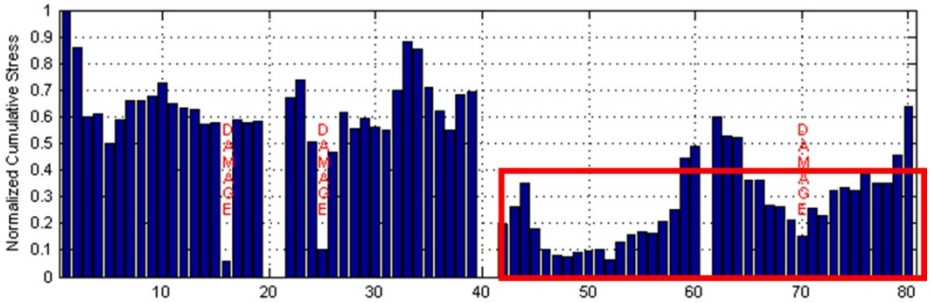

(b) Result of Damage case 1 with C matrix formulation in Eq. (5)

Fig. 4 Simulation results of truss structure 1

Table 1 Results of the substructures in Truss 1

The planar truss 1(20 bays, 81 tubes)	Percentage of measured bays	Percentage of measured tubes	Percentage of measured nodes	Conclusion
Case 1: All nodes are measurements	10% (2 bays/20)	11.11% (9tubes/81)	14.29% (6nodes/42)	Eq. (5) is better
	15% (3 bays/20)	16.05% (13tubes/81)	19.05% (8nodes/42)	Both are good
	20% (4 bays/20)	20.99% (17tubes/81)	23.81% (10nodes/42)	Eq. (4) is better
	>20%	>20.99%	>23.81% (10nodes/42)	Eq. (4) is better
Case 2: Limited nodes are measurements	45% (9 bays/20)	34.57% (28tubes/81)	16.67% (7nodes/42)	Eq. (5) is better
	90% (18bays/20)	71.60% (58tubes/81)	30.95% (13nodes/42)	Eq. (4) is better

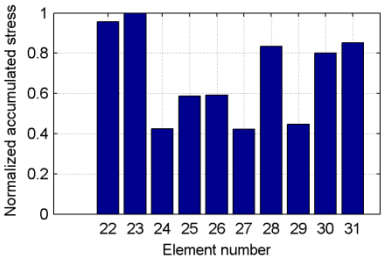

(a) Result of a two-bay substructure using Eq. (4) (element 24 is damaged, 7 measured nodes)

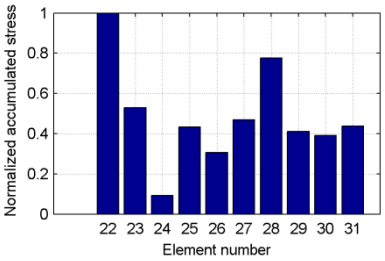

(b) Result of a two-bay substructure using Eq. (5) (element 24 is damaged, 7 measured nodes)

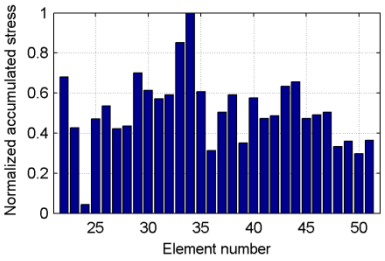

(c) Result of a six-bay substructure using Eq. (4) (element 24 is damaged, 17 measured nodes)

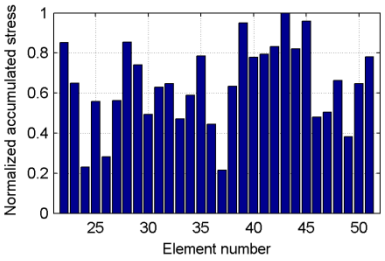

(d) Result of a six-bay substructure using Eq. (5) (element 24 is damaged, 17 measured nodes)

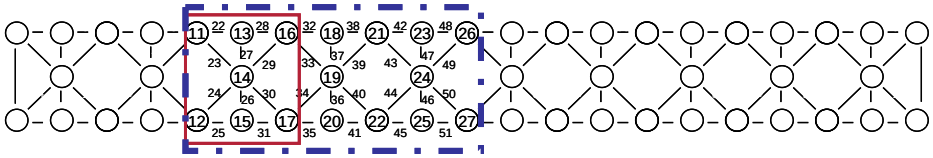

(e) The two-bay substructure and the six-bay substructure in Truss 2

Fig. 5 Simulation results of Truss 2 with damage on Element 24 (5% noise)

Table 2 Results of Truss 1 and Truss 2 based on all nodes in the measured substructures

	Parameter: Percentage of measured nodes	Conclusion
Truss 1 (42 Nodes)	When <= 16.67% (7 measured nodes/42 nodes)	Eq. (5) is better.
	19.05% (8 measured nodes/42 nodes)	Both are good.
	When >= 21.43% (9 measured nodes/42 nodes)	Eq. (4) is better.
Truss 2 (52 Nodes)	When <= 23.08% (12 measured nodes/52 nodes)	Eq. (5) is better.
	25.00% (13 measured nodes/52 nodes)	Both are good.
	When >= 26.92% (14 measured nodes/52 nodes)	Eq. (4) is better.

After the percentage of measured nodes is selected as the final index, the results of truss 1 and truss 2 based on all nodes in the substructure are summarized in Table 2. In Table 2, taking Truss 1 for example, 7 measured nodes could be any combinations in a substructure. For example, they could be nodes {23, 2, 24, 3, 25, 4, 5}, {24, 3, 25, 4, 26, 5, 27}, and so on. Similarly, the 8 measured nodes could be nodes {23, 2, 24, 3, 25, 4, 5}, {24, 3, 25, 4, 26, 5, 27, 6}, and so on. Note that there are some uncertainties in identifying modal parameters using NExT (James, *et al.* 1995) and ERA (Juang and Pappa 1985) technique. To avoid such influence and achieve robust results, both single and multiple damage cases in more than ten substructures, substructures with elements {22 to 31}, {22 to 37}, {22 to 41}, {22 to 42}, {22 to 41, 43, 44}, {22 to 44, 47}, {22 to 47}, {22 to 49}, {22 to 51}, {22 to 57}, {68 to 81}, {82 to 91} and {1 to 102}, are selected as research objects respectively. These damage cases based on different bays are investigated using the two different equations, Eqs. (4) and (5). In addition, every damage case is carried out ten times. The investigation shows the conclusions are not dependent on different selection of substructures. Results in Table 2 are applicable to any substructure in truss 1 or truss 2.

When limited number nodes in a substructure are selected as the measurement nodes (i.e., the sparse sensor layout), numerical results show the same rule as the table 2. Here the sparse sensor layout (Fig. 8) of Truss 2 is used as an example to examine the applicability of the rule in Table 2 for sparse sensor layouts. Table 3 shows the results, it can be seen the threshold of the percentage of measured nodes for the sparse sensor layouts is very close to that in Table 2. The two thresholds are consistent in general.

Note that the conclusions provided in the last column of Tables 1 to 3 are based on the outcome from numerous simulations, according to the criteria given in Section 4.1. For example, the conclusion that Eq. (5) is better than Eq. (4) does not indicate that Eq. (5) always provides better results, but rather than Eq. (5) provides better results in a larger percentage of the simulation outcomes.

Table 3 Results of Truss 2 based on limited number nodes in the measured substructures

	Parameter: Percentage of measured nodes	Conclusion
Truss 2 (52 Nodes)	When <= 21.15% (11 measured nodes/52 nodes)	Eq. (5) is better.
	When >= 23.08% (12 measured nodes/52 nodes)	Eq. (4) is better.

4.3 Selection rule of C matrix

As mentioned previously, the percentage of the measured nodes has been determined as the parameter to select *C* matrix. The simulation results shown in Table 2 indicate that the *C* matrix formulation in Eq. (5) gives more accurate results, on the average, only when Eq. (6) is satisfied, otherwise the *C* matrix formulation in Eq. (4) provides better results, on the average.

$$n_{\text{measured}}/N_{\text{all}} \leq oa \tag{6}$$

where n_{measured} is the number of measured nodes, N_{all} is the number of all nodes in the detected structural plane, and *oa* is a threshold. Also, simulation has shown that the larger the distance between $n_{\text{measured}}/N_{\text{all}}$ and *oa*, the larger probability of obtaining better results using the selected Eq. (4) or Eq. (5). The threshold *oa* varies with structural geometry. For example, *oa* is 19.05% for Truss 1, while it is 25.00% for Truss 2. To find the threshold value of *oa*, some numerical simulation based on the detected structure should be implemented first.

Nagayama *et al.* (2009) give a conclusion based on some 2-bay substructures of a truss structure (their paper shows results based on five different two-bay substructures): the *C* matrix formulation in Eq. (5) gives more accurate results than using Eq. (4). Actually, this conclusion is consistent with the conclusion in Eq. (6) of this work. That is because in the work of Nagayama *et al.* (2009), a two-bay substructure has 6 measured nodes and the truss has 28 nodes in all, so $n_{\text{measured}}/N_{\text{all}} = 6/28 = 21.43\%$, which is less than the threshold; however, for damage detection of a 5-bay substructure in the work of Nagayama *et al.* (2009), the *C* matrix formulation in Eq. (4) gives more accurate results than using Eq. (5) in about 80 runs out of 100 simulations; for damage detection of a 7-bay substructure, the *C* matrix formulation in Eq. (4) gives more accurate results in about 90 runs out of 100 simulations.

From singular value decomposition (SVD), one can get

$$dQ = \Delta Q = USV^T = \begin{bmatrix} U_1 & U_0 \end{bmatrix} \begin{bmatrix} S_1 & 0 \\ 0 & 0 \end{bmatrix} \begin{bmatrix} V_1 & V_0 \end{bmatrix}^T \tag{7}$$

According to the definition of SVD decomposition, *V* should be a unitary matrix. Because the real analogue of a unitary matrix is an orthogonal matrix, the unitary matrix *V* becomes an orthogonal matrix when its imaginary parts are zero. According to the SDLV method, the damage locating vectors should be the real part of the complex matrix V_0 (last several columns in complex matrix *V*); *V* should be a complex matrix; in other words, *V* should be a unitary matrix (complex) not an orthogonal matrix (real). From the formulations of Eqs. (4) and (5), one can see Eq. (4) has more information than Eq. (5), so generally, Eq. (4) should be used to identify the damage. However, when Eq. (4) is used to calculate the *dQ* matrix using Eq. (1), *dQ* is close to a real matrix since its imaginary part are close to zero; thus, *V* matrix may not be a complex matrix. Based on our initial analysis, the threshold used in the selection of the *C* matrix is related to the SVD. When Eq. (4) is used, the *V* matrix has a property which is related to the size of the complex d*Q* matrix:

1) When the size of *dQ* matrix is smaller than a threshold, after SVD, the imaginary parts of all column vectors in *V* are zero, so *V* is an orthogonal (real) matrix, not a complex matrix. When such a *V* matrix based on Eq. (4) is used in the damage detection, the result is inferior to that using Eq. (5). Therefore, Eq. (5) should be used to get more accurate result. Further work needs to be done to better understand why the results based on Eq. (5) are better when the size of *dQ* matrix is smaller than the threshold.

2) However, as the size of the *dQ* matrix increases, the imaginary parts of the last several columns in the *V* matrix become nonzero. The number of nonzero columns increases as the size of the *dQ* matrix increases. In such cases, *V* is a unitary matrix and the real part of *V* is no longer an orthogonal matrix. When such a *V* matrix based on Eq. (4) is used in the damage detection, the result is more accurate than using Eq. (5). One possible explanation is that when the size of *dQ* increases, i.e. the size of φ_i (i = 1, 2, …, n, see Eqs. (4) and (5)) increases, when the size is greater than a threshold, Eq. (5) loses too much information compared with Eq. (4).

The threshold for the size of *dQ* matrix is consistent with the threshold of the percentage of measured nodes as proposed in this paper. When Eq. (4) is employed in the calculation of *dQ* using Eq. (1), the property of *V* matrix from SVD of *dQ* is changing with the size of *dQ*. The objective of section 4 (i.e., main focus 1) is to show the relationship between damage detection results and the *C* matrix formulations in Eqs. (4) and (5); also, section 4 gives the rule to select *C* matrix formulation in order to get better results.

5. Main focus 2: study about the proposed strategies of sensor layout

A suitable strategy of sensor layout is critical to effective damage detection with limited number of sensors. The strategy of sensor layout decides the number and position of sensors, and it is related to the structural geometry. The strategies of sensor layout of truss bridges with two common structural forms are studied in this section.

5.1 The flow of damage localization

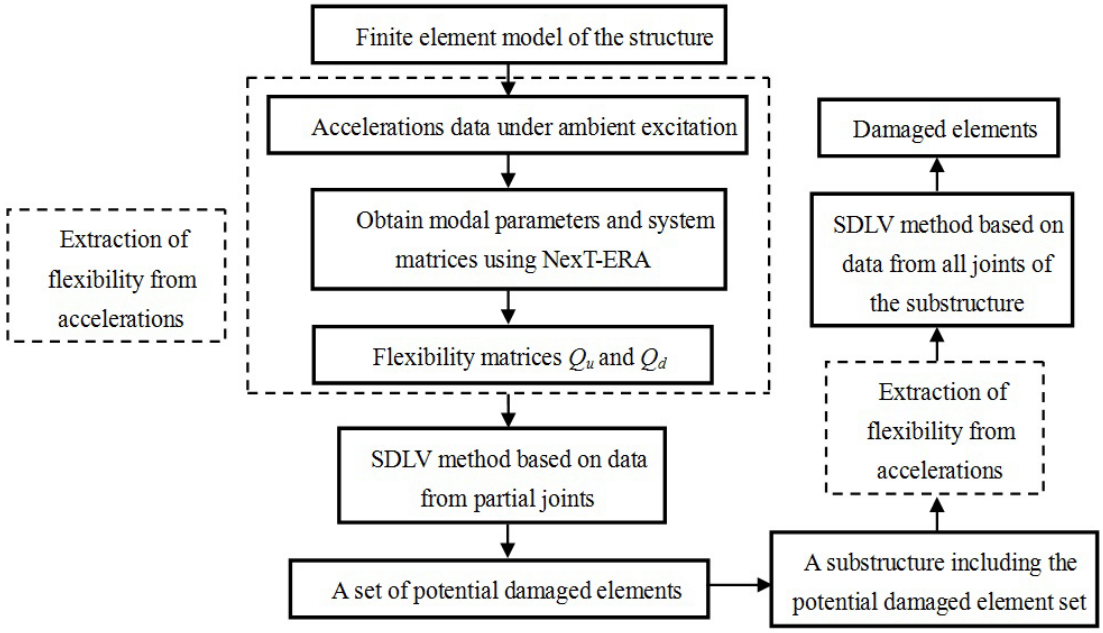

Fig. 6 Flowchart of damage localization

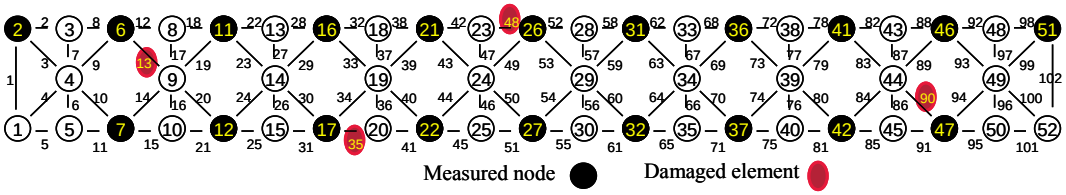

Fig. 7 The first proposed strategy of sensor layout

Sensors are an important part in SHM system, once the number of sensors increases, cost of the corresponding data acquisition system and the subsequent maintenance will increase. In order to decrease the cost of the SHM system, limited sensors should be employed in engineering from an economic perspective. On the other hand, the SDLV method can detect the damage mainly based on the change of flexibility matrices before and after damage. When all nodes in the detected structure or substructure are selected as measured nodes, the dimension of the square matrix ΔQ^T is 2 times (two directional measurements) of the number of measured nodes, then the information from the closest two nodes will change when some element is damaged, the corresponding information in the damaged flexibility matrix of the two nodes will change, finally the damage can be detected after SDLV algorithm is employed. However, when limited sensors of the detected structure or substructure are used to build the flexibility matrix, the SDLV method can only tell the damaged section which contains the damaged elements and false positives. Thus, if the exact damaged elements are required, the second step of damage detection should be conducted again in the damaged section with measured nodes from all nodes in this section. Therefore, a two-step damage localization procedure is shown in the flowchart in Fig. 6.

5.2 The proposed three strategies of sensor layout for bailey truss structures

As shown in Figs. 7-9, three strategies of sensor layout are proposed for detecting damaged elements of the truss structure. It should be noted that the proposed sparse sensor layouts are incomplete; they are only three alternative strategies. While the sensor layout using a limited number of sensors may not identify the exact damage location, it can detect damage between two sensors. The reasons for investigating these three sensor layouts are described as follows:

For the first strategy of sensor layout (Fig. 7),

(1) The most important elements in the truss structure are the upper and lower cord elements. Therefore, in the first sensor layout, sensors are placed on the nodes along the upper and lower cords to monitor potential damage on these most important elements.

(2) To achieve balance between accuracy (false positive results) and cost (number of sensor nodes), sensors are placed with one node interval. In this case, according to the simulation result (for example, Fig. 10), whenever a single upper/lower cord is damaged, the other element located between the same pair of sensors will also be identified as damaged element, causing one false-positive result. The result can be explained by force balance since these two horizontal elements are balancing each other due to the fact that no sensor is placed between them and hence no force from the DLVs is applied between them. For example, in the first sensor layout, node 20 are connected by three elements, when element 35 is damaged, element 41 must has zero stress to achieve force balance.

(3) With this sensor layout, the diagonal elements, which are also important elements for this truss bridge, are also monitored in the same manner as the lower and upper cord elements, i.e., two diagonal elements (e.g., elements 13 and 20) are monitored by two sensors (e.g., sensors 6 and 12), and whenever one of the two elements is damaged, the other one will also be identified damaged, according to simulation results (Fig. 10).

For the second strategy of sensor layout (Fig. 8),

(1) As we can see, the first sensor layout will always have one false positive result for both upper/lower cord and diagonal elements. To increase the accuracy for the upper/lower cord elements, the second sensor layout is therefore proposed by shifting the locations of the sensors. This sensor layout has identical number of sensors as in the first layout.

(2) The advantage of the second sensor layout, according to the simulation result, is that the damaged elements in the upper/lower cord can be identified accurately, i.e., no false positive results. The reason is that the unmeasured nodes on the upper/lower cord (for example, node 17) are now connected by four elements; when one horizontal element (for example, element 35) is damaged, the remaining three elements can still achieve force balance.

(3) The disadvantage of the second sensor layout is that the accuracy of damage detection for diagonal elements is lower than the first sensor layout. Based on simulation results, if one diagonal element is damaged, the other three elements in the same bay will also be identified as damaged elements, causing three false positive results. For example, when element 19 is damaged, elements 19, 20, 23, and 24 are all identified as damaged. Although force balance can only explain the zero force in element 23, we found that this specific sensor layout and structural geometry will introduce a specific set of DLVs which also cause low force in elements 20 and 24.

For the third strategy of sensor layout (Fig. 9),

(1) As we can see, all the diagonal elements are connected by the intermediate nodes such as 4, 9, and 14. The third sensor layout is therefore proposed by using all these intermediate nodes and several nodes on the upper and lower cords to monitor the diagonal elements and the horizontal elements in the structure.

(2) If one upper/lower cord element is damaged, the other upper/lower cord element with the same ‘T’ intersection node will be a false positive element. For example, element 41 will be a false positive element when element 35 is damaged. The reason is that the unmeasured nodes on the upper/lower cord (such as node 20) are now connected by three elements including one vertical element and two horizontal elements; when one horizontal element (such as element 35) is damaged, the other horizontal element must have a zero stress to achieve force balance. However, the unmeasured nodes on the upper/lower cord (such as node 17) are now connected by four elements; when one horizontal element (such as element 35) is damaged, the remaining three elements can achieve force balance, so the element 31 is not a false positive element when element 35 is damaged.

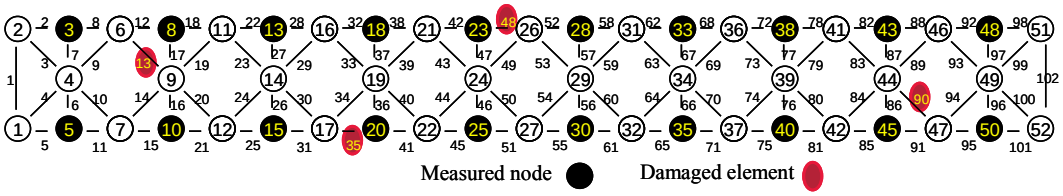

Fig. 8 The second proposed strategy of sensor layout

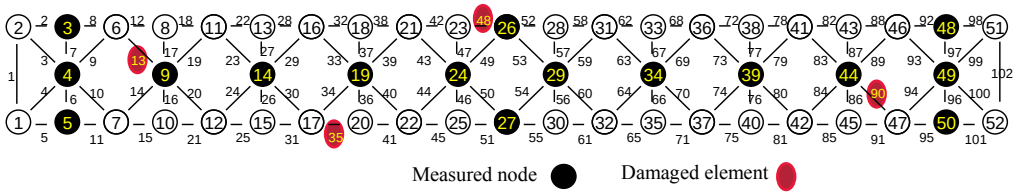

Fig. 9 The third proposed strategy of sensor layout

(3) If one upper/lower diagonal element is damaged, the other upper/lower diagonal elements in the same bay will be false positive elements. The reason is that the unmeasured nodes on the upper/lower cord (such as node 6) are now connected by four elements including two horizontal elements and two upper/lower diagonal elements; when one upper/lower diagonal element (such as element 13) is damaged, the other upper/lower diagonal element (such as element 9) must have a zero stress to achieve force balance.

In summary, all the three sensor layouts are designed to monitor the important upper/lower cord and diagonal elements in the truss bridge, with considerations trying to balance the accuracy and cost. All layouts have pros and cons in terms of damage detection accuracy. Both the first and third sensor layouts have one false positive result associated with a single damaged element for both upper/lower cord elements and diagonal elements. However, the second sensor layout has no false positive result for upper/lower cord elements (accurate identification) but three false positive results for diagonal elements associated with one damaged element.

5.3 Damage case 2 based on the first strategy of sensor layout

The truss (Fig. 7) is excited using a band-limited white noise up to 200 Hz in the vertical direction at node 37. A band-limited white noise with RMS amplitude about 5% of the measured signal is added to simulate measurement noise. The sampling frequency for measurement is 500 Hz.

5.3.1 Damage localization

Damage case 2 is a multiple damage case: elements 13, 35, 48 and 90 in truss 2 have 50% stiffness reduction, which are used to simulate the damage of the upper diagonal truss member, the lower chord, the upper chord, and the lower diagonal truss member, respectively. The entire planar structure is selected as the damage detection objective, and the 20 black nodes shown in Fig. 7 are selected as measurements. Thus the percentage of the number of measured nodes is 20/52 > 23.08% (Table 3); therefore, Eq. (4) should be used to calculate C matrix according to Table 3.

One issue is that the threshold limit of *WSI* is recommended to a number not great than b, and b = 0.1 in the study of Bernal (Bernal 2002). The threshold value depends on various parameters such as the form of the detected structure. A threshold value of b = 0.2 is recommended in this work. In accordance with the aforementioned steps (Fig. 6), ten identifications have done based on different noise data. The average value (selecting average value avoids the possible mistake and reduces the effect of some corrupted data) of the ten results are obtained respectively as the final result of Damage case 2 (Fig. 10), in which eight elements have a normalized cumulative stress less than 0.2. Besides the 4 damaged elements, the result also contains 4 false positive elements 20,

41, 42 and 83 (Fig. 10). The result is not consistent with the real case due to some false positive results, but the locations of the damaged elements are placed symmetrically in the result. Results in this step are regarded as the potentially damaged elements.

5.3.2 Result analysis

Some false positive elements presented in the result of Damage case 2. A possible explanation is that the false positives may happen more frequently if the number of measurements is further reduced. However, many numerical results show that the potentially damaged elements are present in couples, and the potentially damaged elements are placed at symmetrical locations in every couple. As shown in Fig. 11, element a2 (a4) will be false positive element when element a1 (a3) is damaged; element b2 (b4) will also be false positive element when element b1 (b3) is damaged, and vice versa. This is determined by the structural geometry of the bailey steel-truss bridge and the strategy of sensor layout. Certainly, it is possible that the potentially damaged elements are all damaged. To obtain the real damaged elements, a substructure including the potentially damaged elements should be detected again by the SDLV method based on data from all nodes of the substructure or physics tests. Although damaged elements have not been detected directly due to some false positive elements, the sensor layout is still successful to obtain the potentially damaged elements.

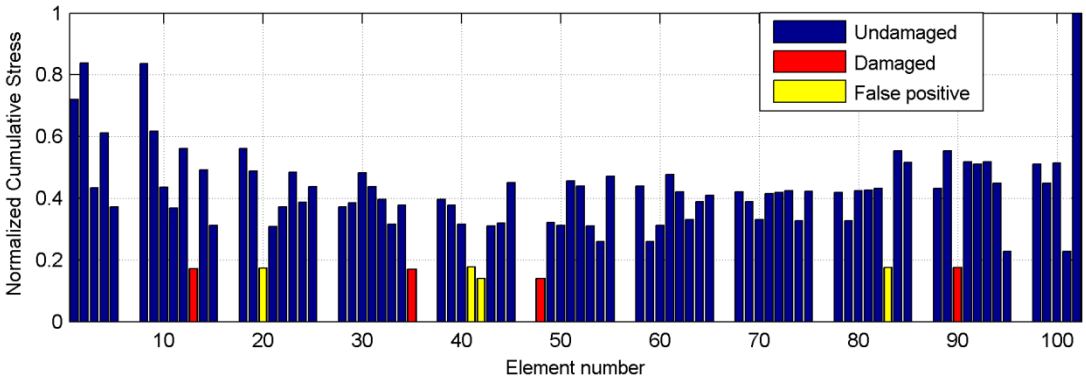

Fig. 10 Result of Damage case 2 based on the first strategy of sensor layout (5% noise)

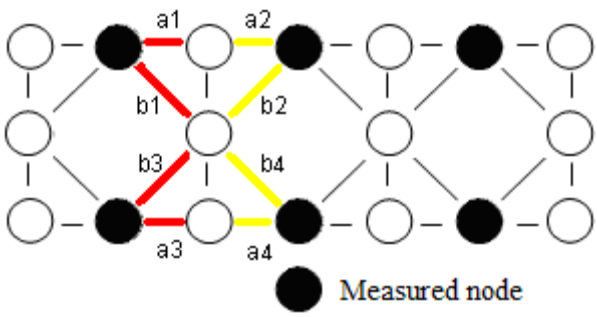

Fig. 11 Illustration of results for the first strategy of sensor layout

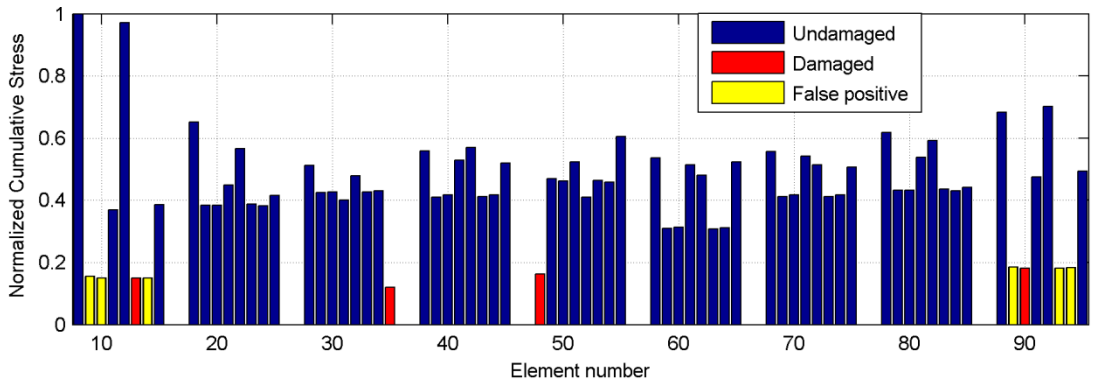

Fig. 12 Result of damage case 2 based on the second strategy of sensor layout (5% noise)

5.4 Damage case 2 based on the second strategy of sensor layout

5.4.1 Damage localization

20 nodes (the black ones in Fig. 8) are selected as measurements of Damage case 2 in this strategy. The average value of ten detection results is obtained as the final result (Fig. 12), in which ten elements have a normalized cumulative stress less than 0.2 (the threshold). The result also contains six misidentifications of 9, 10, 14, and 89, 93, 94 (Fig. 12). But the potentially damaged elements based on the second strategy of sensor layout are still present regularly.

5.4.2 Result analysis

(1) The simulation results show that the exact location of the upper (such as a1 and a2 in Fig. 11) and lower such as a3 and a4 in Fig. 11) chord truss elements in the structure can be detected directly based on the SDLV method with the second strategy.

(2) When one diagonal truss member is damaged, the other diagonal ones in the same bay are also identified as damaged whether they are damaged or not. As shown in Fig. 13, all of elements b1, b2, b3, and b4 will be present in the result when one or more than one of them are damaged.

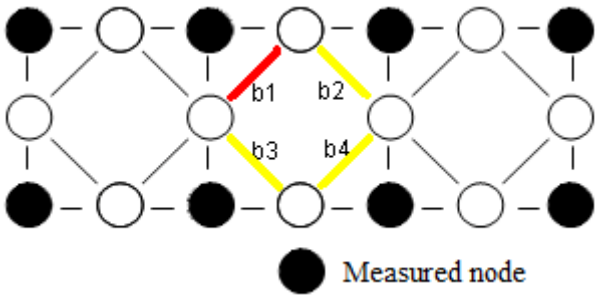

Fig. 13 Illustration of results for the second strategy of sensor layout

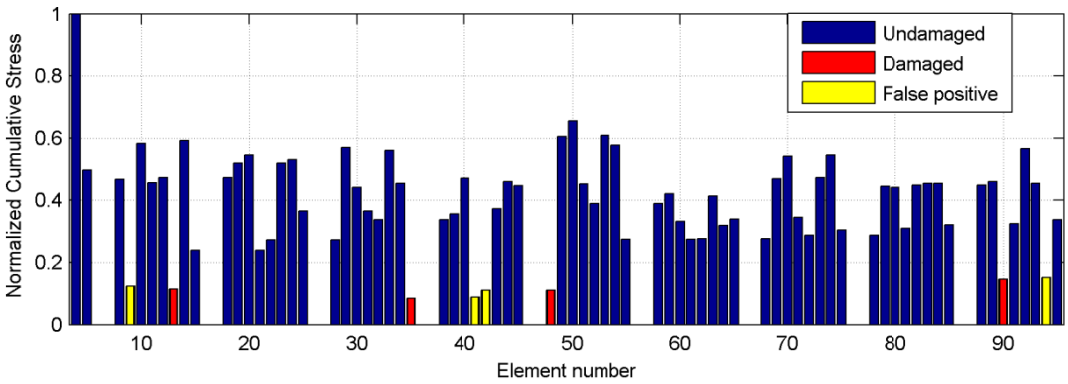

Fig. 14 Result of damage case 2 based on the third strategy of sensor layout (5% noise)

5.5 Damage case 2 based on the third strategy of sensor layout

5.5.1 Damage localization

Here, 16 nodes (the black ones in Fig. 9) are selected as the measurement nodes in the third strategy. The number of measured nodes is less than one third of the total number of nodes. The average value of ten damage detection results is obtained as the final result (as shown in Fig. 14), in which eight elements have a normalized cumulative stress less than 0.2. The result contains four false positive elements of 9, 41, 42 and 94 (Fig. 14), and the potentially damaged elements based on the third strategy of sensor layout are still present regularly.

5.5.2 Result analysis

The simulation results based on the third strategy show that:

(1) For the upper and lower chord truss elements, when element a1 (a3) is damaged, element a2 (a4) will be false positive element, and vice versa.

(2) For the diagonal truss elements, when element b1 (b3) is damaged, element b2 (b4) will be false positive element, and vice versa.

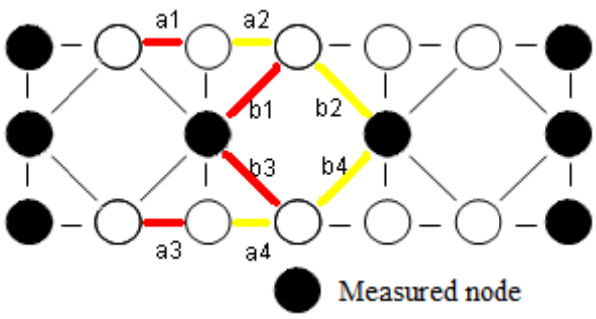

Fig. 15 Illustration of results for the third strategy of sensor layout

5.6 Diagnosis of the potential damaged elements

To obtain the real damaged elements, the substructure including all potentially damaged elements can be detected again by the SDLV method based on data from all nodes within the substructure. Damage detection of the substructure in Fig. 16(a) is implemented here assuming that elements 35 and 41 in the ellipse are the potentially damaged elements, but actually, only element 35 is damaged with 50% stiffness reduction, which is damage case 3. Four nodes in the substructure are selected as measured nodes. Numerical simulation showed that the *C* matrix in Eq. (5) can give better damage detection results here. The result (Fig. 16(b)) indicates that the final damaged element is 35, while element 41 is a misidentification.

5.7 The strategy employed in another common type of truss structure (Truss 1)

The numerical example of Damage case 1 in Truss 1 is used to test the strategy on a different type of truss structure. The strategy of sensor layout is shown in Fig. 17 to identify Damage case 1. 13 nodes (the black nodes in Fig. 17) are selected as measurements. The sampling frequency is 500 Hz. The amplitude of measurement noise is 5%. The results are shown in Fig. 18, in which six elements have a normalized cumulative stress less than 0.2 (the threshold). The result contains both the damaged elements 16, 25, and 70, and the undamaged elements 15, 24, and 69 (the misidentifications in Fig. 18). It is still clear that damaged elements are present in couples, and they are placed at symmetrical locations. 72% of the truss members of the structure can be detected, even though only 31% of the nodes are utilized as measurements.

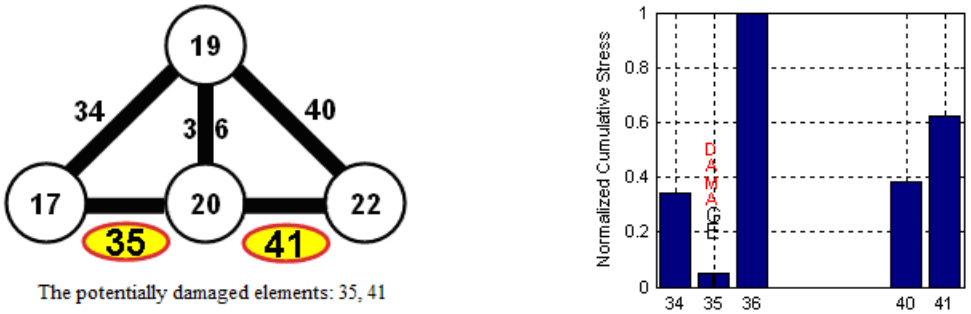

(a) (b)

Fig. 16 (a) The substructure for damage case 3, (b) Result based on data from all nodes of the substructure

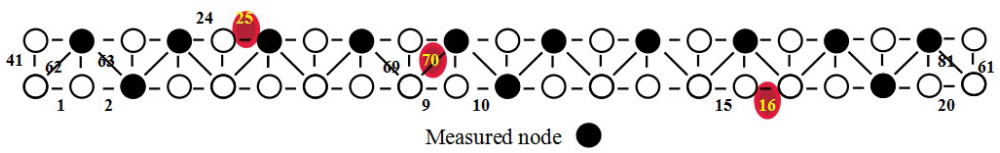

Fig. 17 The strategy of sensor layout for Truss 1 (Damage case 1)

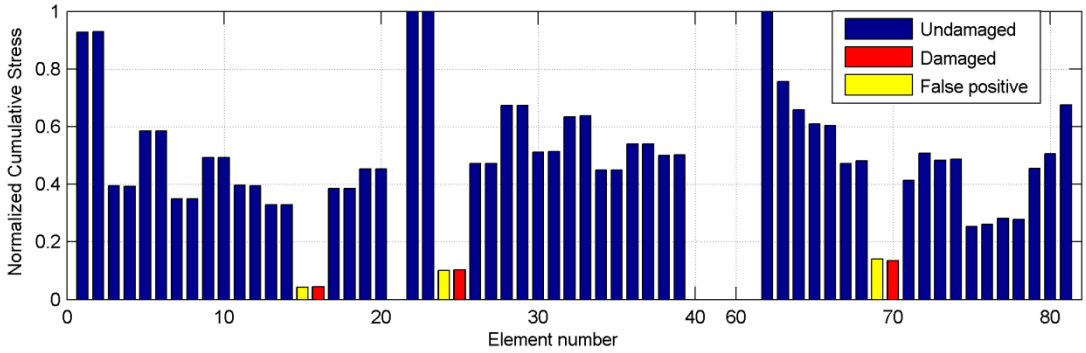

Fig. 18 Result of Damage case 1 based on the proposed strategy of Truss 1

Table 4 Some results based on data from partial nodes of substructures from Trusses 1 and 2

	Parameter: Percentage of measured nodes	Conclusion
Truss 1	16.67% (7 measured nodes/42 nodes)	Eq. (5) is better.
(42 Nodes)	30.95% (13 measured nodes/42 nodes)	Eq. (4) is better.
Truss 2	19.23% (10 measured nodes/52 nodes)	Eq. (5) is better.
(52 Nodes)	38.46% (20 measured nodes/52 nodes)	Eq. (4) is better.

5.8 Applicability of the selection rule of C matrix for the proposed strategies

The selection rule of *C* matrix is still applicable to the proposed strategies of sensor layout which only employs partial nodes of the detected structure or substructure. Some results based on data from partial nodes of substructures from Trusses 1 and 2 are shown in Table 4, from which one can see the results are still consistent with the proposed rule in 4.3 though they are based on limited nodes of the substructures.

6. Main focus 3: Sensitivity analysis of the method to different types of truss members

To investigate the relationship between the successful rate of damage localization results and damage severity for different types of truss elements, i.e., vertical, horizontal and diagonal elements, focus 3 is discussed here. Due to the randomness of the noise, identification results are uncertain with slight variations even with the same noise level. Many simulation results show that:

(1) The successful rate of localization results increases with the increase of damage severity;

(2) The sensitivities of the SDLV method to different types of truss elements are distinctly different: to get the same successful rate of results and the critical damage severities are different for different types of truss elements.

Taking Truss 2 for example, results of a substructure (including elements 22 to 31) when

different types of truss elements are damaged respectively are shown in Table 5. In many damage identifications based on different sets of data from a damage case, the following damage severities must be given in order to get 90% successful rate of the results: the vertical truss element 26 must be given 70% stiffness reduction, the longitudinal truss element 25 must be given 50% stiffness reduction, and the diagonal truss element 24 only needs about 25% stiffness reduction. Here 90% successful rate means there are about 90% results are correct in multiple identifications based on different sets of data, for example, there are 9 accurate results in 10 identifications of the same damage case.

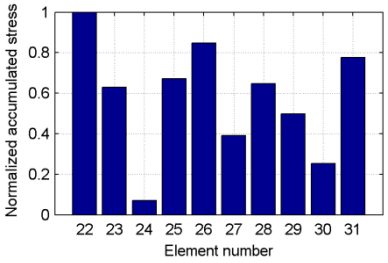

(a) Element 24 is damaged with 25% stiffness reduction

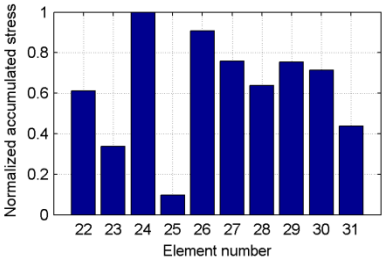

(b) element 25 is damaged with 50% stiffness reduction

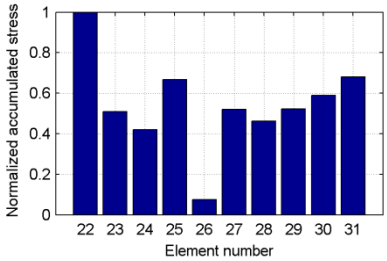

(c) element 26 is damaged with 70% stiffness reduction

Fig. 19 Simulation results of a substructure from Truss 2 (5% noise)

Table 5 Simulation results of Truss 2 for damage of different types of truss members

Types of truss members	Reduction of Young's modulus	Successful rate of results
The diagonal element 24	25%	90%
The longitudinal element 25	25%	30%
	50%	90%
The vertical element 26	25%	10%
	70%	90%

7. Experimental verification

To verify that the proposed strategies of sensor layout are feasible, experiments of the same substructure for single and multiple damage cases are implemented respectively. As shown in Fig. 20(a), eight nodes (nodes 1 to 8) are selected as measurements to detect the substructure based on the second strategy of sensor layout. The bidirectional accelerations before damage are obtained from the experimental model or the SIMULINK model. Damage case 4 is a single damage case, in which the lower diagonal truss member 70 is replaced with one that has a reduced thickness (Fig. 21(b)). Damage case 5 is a multiple damage case, in which the original lower diagonal truss member 49 is replaced with one that is grooved (Fig. 21(a)) besides the damaged member 70.

7.1 Damage localization experiment

A band-limited white noise is sent from the computer to the shaker to excite the truss model up to 120 Hz in the vertical direction at nodes 17 to simulate ambient excitation. The sampling frequency is 500 Hz. The Dynamic Systems magnetic JZK-10 shaker (Fig. 22(a)) from Sinocera Piezotronics Inc. can generate a maximum force of 100N, and the accelerometers from Lance technologies Inc. have a sensitivity of 1527~2048 mV/g and a frequency range of 0.1 to 2000 Hz. A data acquisition PXI system from National Instruments was used to collect the accelerations. The bidirectional (or one vertical and one longitudinal) accelerometers are installed on the measured joints.

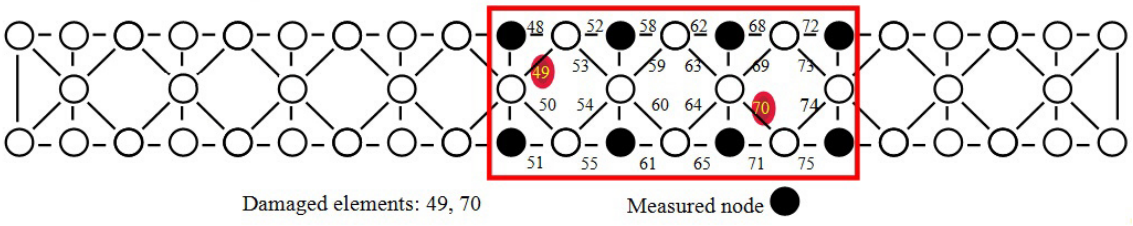

(a)

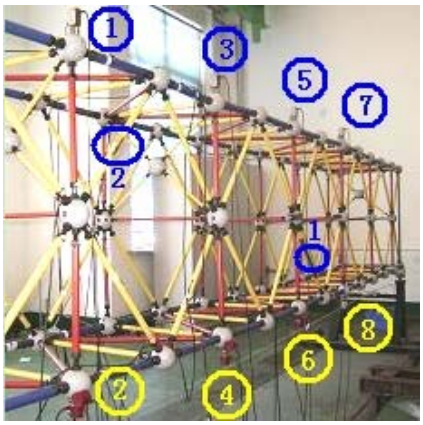

(b)

(c)

Fig. 20 (a) Damage case 5 (the substructure in the rectangle is the experimental object), (b) damage case 5 in the experimental model and (c) the bidirectional accelerometer

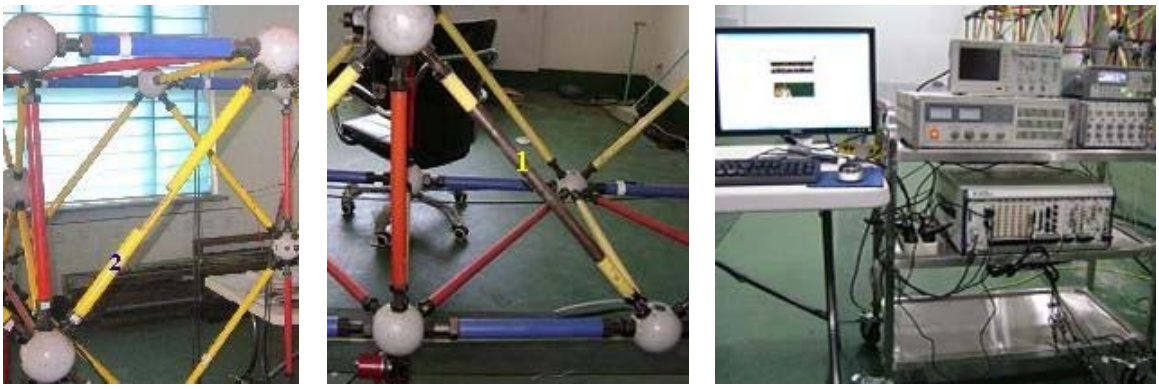

(a) (b) (c)

Fig. 21 (a) The damaged member 49, (b) The damaged member 70 and (c) Experimental test system

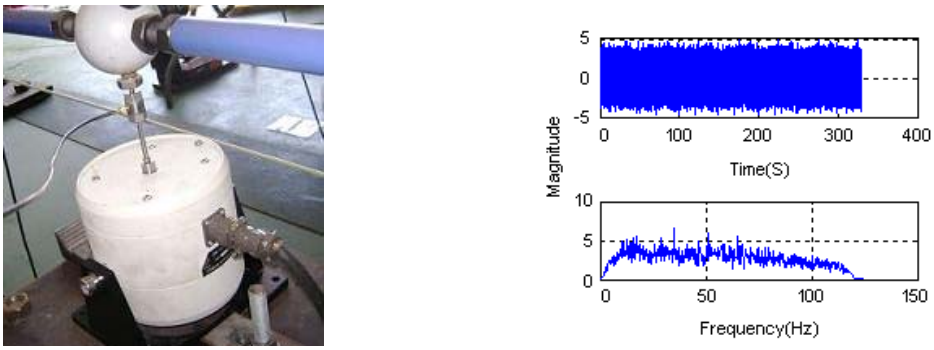

(a) (b)

Fig. 22 (a) The magnetic shaker and (b)The white noise signal from magnetic shaker

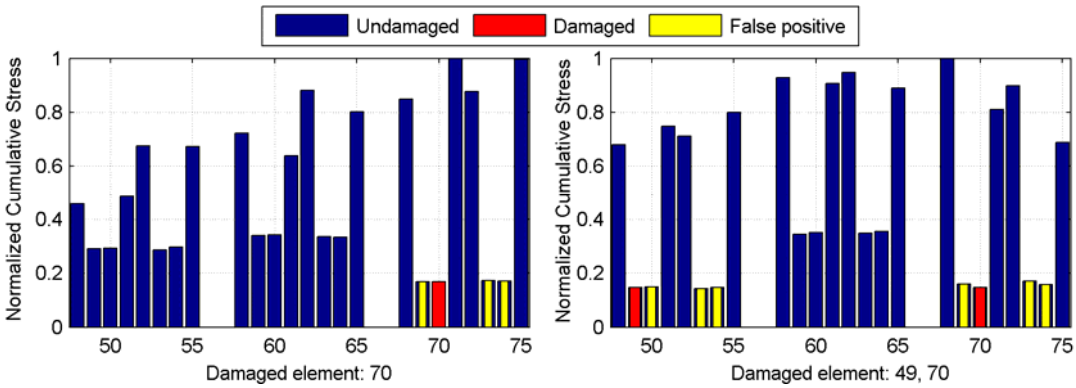

Fig. 23 Result of Damage cases 4 and 5 based on the second strategy

Damage case 4 and 5 based on the second strategy of sensor layout are implemented respectively. The results are shown in Fig. 23, in which the experimental results contain both the damaged elements and the misidentifications. The experimental results agree well with the simulation since the potentially damaged truss members are detected.

7.2 Diagnosis of the potential damaged truss members

After the potentially damaged truss members are detected successfully, the substructure including all potentially damaged elements can be detected again by the SDLV method based on data from all nodes of the substructure (such as Fig. 16) or physics test to obtain the real damaged truss members. Then, all misidentifications can be excluded from the potentially damaged truss members.

8. Conclusions

In this paper, the "DUT steel-truss bridge Benchmark Model" and the other common type of truss structure have been selected as research objects; three focuses have been completed: to study the influence of difference formulation of the *C* matrix on the accuracy of damage detection results in SDLV method; to propose and verify three strategies of sensor layout for truss structures with a limited number of sensors for SDLV method; to investigate the relationship between the accuracy of damage detection results and damage severity for different types of truss elements. The conclusions can be summarized as follows:

(1) The damage localization results are directly related to the formulation of the *C* matrix, and the selection rule is closely related to the percentage of the measured nodes. The threshold of the percentage of measured nodes, i.e., *oa*, can be recommended according to the simulation of the detected structure.

(2) Both simulation and experimental results of the bailey truss model show that the most important truss members can be detected successfully by utilizing the proposed strategies of sensor layout. The work also gave the suitable strategies based on the SDLV method for another common truss structure. With these strategies, the number of sensors employed in the SHM of truss drastically drops, which can greatly reduce the costs and workload in engineering.

(3) The accuracy of damage localization will increase with the increase of damage severity. The sensitivities of the SDLV method to different types of truss elements are distinctly different, i.e., in order to get the same accuracy of localization results, the critical damage severities are different for different types of truss elements.

Acknowledgments

The authors are grateful for the financial support from the Fundamental Research Funds for the Central Universities of China, the National Key Technology R&D Program of China (Grant No. 2011BAK02B01 & 2011BAK02B03) and the National Natural Science Foundation of China (Grant No. 51161120359). The first author appreciates the support from China scholarship council and the help from Stephanie Tong (the University of Illinois at Urbana-Champaign). Moreover, special thanks to Bernal D. for the studies of SDLV method.

References

An, Y.H. and Ou, J.P. (2010), "Research on a long-span truss steel bridge Benchmark model for health monitoring", *Proceedings of the 19th national Bridge Conference (China)*, Shanghai, June, 1284-1291 (in Chinese).

An, Y.H. and Ou, J.P. (2012), "Experimental and numerical studies on damage localization of simply supported beams based on curvature difference probability method of waveform fractal dimension", *J. Intel. Mat. Syst. Str.*, **23**, 415-426.

An, Y.H. and Ou, J.P. (2013), "Experimental and numerical studies on model updating method of damage severity identification utilizing four cost functions", *J. Struct. Control Health Monit.*, **20**(1), 107-120.

Bernal, D. (2006), "Flexibility-based damage localization from stochastic realization results", *J. Eng. Mech. - ASCE*, **132**(6), 651-658.

Bernal, D. (2002), "Load vectors for damage localization", *J. Eng. Mech. - ASCE*, **128**(1), 7-14.

Balmès, E., Basseville, M., Mevel, L., Nasser, H. and Zhou, W. (2008), "Statistical model-based damage localization: A combined subspace-based and substructuring approach", *Struct. Control Health Monit.*, **15**(6), 857-875.

Caicedo, J.M., Dyke, S.J. and Johnson, E.A. (2004), "Natural excitation technique and eigensystem realization algorithm for phase I of the IASC-ASCE benchmark problem: simulated data", *J. Eng. Mech. - ASCE*, **130**(1), 49-60.

Chen, B.L. and Nagarajaiah, S. (2008), "Structural damage detection using decentralized controller design method," *Smart Struct. Syst.*, **4**(6), 779-794.

Deraemaeker, A., Preumont, A., Reynders, E., De Roeck, G., Kullaa, J., Lamsa, V., Worden, K., Manson, G., Barthorpe, R., Papatheou, E., Kudela, P., Malinowski, P., Ostachowicz , W. and Wandowski, T. (2010), "Vibration-based structural health monitoring using large sensor networks", *Smart Struct. Syst.*, **6**(3), 335-347.

Gao, Y. (2005), *Strctural health monitoring strategies for smart sensor networks*, PhD Thesis, Graduate College of the University of Illinois at Urbana-Champaign, U.S.A.

Gao, Y., Spencer Jr, B.F. and Bernal, D. (2007), "Experimental verification of the flexibility-based damage locating vector method", *J. Eng. Mech. - ASCE* , **133**(10), 1043-1049.

Hu, N., Wang, X., Fukunaga, H., Yao, Z.H., Zhang, H.X. and Wu, Z.S. (2001), "Damage assessment of structures using modal test data", *Int. J. Solids Struct.*, **38**(18), 3111-3126.

James, G.H., Carne, T.G. and Lauffer, J.P. (1995), "The natural excitation technique (NExT) for modal parameter extraction from operating structures", *J. Anal. Expert. Modal Anal.*, **10**(4), 260-277.

Juang, J.N. and Pappa, R.S. (1985), "An eigensystem realization algorithm for modal parameter identification and model reduction", *J. Guid. Control Dynam.*, **8**(5), 620-627.

Katkhuda, H. and Haldar, A. (2008), "A novel health assessment technique with minimum information", *Struct. Control Health Monit.*, **15**(6), 821-838.

Kim, H. and Melhem, H. (2004), "Damage detection of structures by wavelet analysis", *Eng. Struct.*, **26,** 7-14.

Lifshitz, J.M. and Rotem, A. (1969), "Determination of reinforcement unbonding of composites by a vibration technique", *J. Compos. Mater.*, **3**(3), 412-423.

Mathwork Inc. (2005), *Matlab user manual,* Lowell, MA, U.S.A.

Nagayama, T., Spencer Jr, B.F. and Rice, J.A. (2009), "Autonomous decentralized structural health monitoring using smart sensors", *Struct.Control Health Monit.*, **16**(7-8), 842-859.

Ou J.P. (2005), "Research and practice of smart sensor networks and health monitoring systems for civil infrastructures in mainland China", *Bulletin of National Science Foundation of China*, **19**(1), 8-12 (in Chinese).

Pandey, A.K., Biswas, M. and Samman, M.M. (1991), "Damage detection from changes in curvature mode shapes", *J. Sound Vib.*, **145**(2), 321-332.

Pandey, A. and Biswas, M. (1996), "Damage detection in structures using changes in flexibility", *J. Sound*

Vib., **169**(1), 3-17.
Shi, Z.Y., Law, S.S. and Zhang, L.M. (2000), "Structural damage detection from modal strain energy change", *J. Eng. Mech.- ASCE*, **126**(12), 1216-1223.
Yan, Y.J., Cheng, L., Wu, Z.Y. and Yam, L.H. (2007), "Development in vibration-based structural damage detection technique", *Mech. Syst. Signal Pr.*, **21**, 2198-2211.
Yu, L.Y. and Giurgiutiu, V. (2005), "Advanced signal processing for enhanced damage detection with piezoelectric wafer active sensors", *Smart Struct. Syst.*, **1**(2), 185-215.
Zhou, D., Ha, D.S. and Inman D.J. (2010), "Ultra low-power active wireless sensor for structural health monitoring", *Smart Struct. Syst.*, **6**(5-6), 675-687.
Zhou, L., Yuan, F.G. and Meng, W.J. (2007), "A pre-stack migration method for damage identification in composite structures", *Smart Struct. Syst.*, **3**(4), 439-454.

BS